Finite element analysis of some concrete non-linearities: theory and examples

IABSE
AIPC
IVBH

SEMINAR on:
«CONCRETE STRUCTURES SUBJECTED TO TRIAXIAL STRESSES»
17th-19th MAY, 1974 - ISMES - BERGAMO (ITALY)

III-2

Finite element analysis of some concrete non-linearities Theory and examples

Analyse par éléments finis de quelques non-linéarités relatives aux ouverages en béton - Théorie et examples

Analyse Begrenzter Elemente einiger nichtlinearer Betonarten - Darstellung der Theorie mit Beispielen

O. C. ZIENKIEWICZ,
Professor of Civil Engineering,
University of Wales,
Swansea, U. K.

D. V. PHILLIPS,
Lecturer, Dept. of Civil Engineer-
ing, University of East Africa,
Nairobi, Kenya (formerly of Uni-
versity of Wales, Swansea, U.K.)

D. R. J. OWEN,
Lecturer, Dept. of Civil
Engineering, University of
Wales, Swansea, U. K.

INTRODUCTION

For most engineering situations the assumption of linear elastic behaviour for reinforced concrete provides results which are adequate for design purposes. Indeed in the past the limitations imposed by analytical techniques have generally made such an assumption essential. However in some cases the inclusion of non-linear effects is of paramount importance and this is becoming increasingly so with emphasis gradually shifting to "limit state" design for improved structural efficiency.

The development of numerical techniques, such as the finite element method, has enabled material non-linearities to be readily included in analysis and the parallel development of high speed digital computers has ensured that solutions can be obtained to practical engineering problems at an economical cost.

The non-linear behaviour of reinforced concrete arises from the non-linear action of the individual constituents. Undoubtedly the prime cause of non-linearity in most structures is the inability of concrete to sustain tensile loading, with crack development and load redistribution occurring with increasing load. Such behaviour imposes severe demands on any non-linear solution technique due to the extreme strain softening nature of crack development. A secondary source is the non-linear response of concrete under multiaxial compressive stress states. However despite intensive and continued research no universally accepted constitutive law exists at present which fully describes the above two phenomena under fully three-dimensional stress conditions. On the other hand, the behaviour of the steel reinforcement after yielding is adequately described by the classical theory of plasticity.

2.

(a)
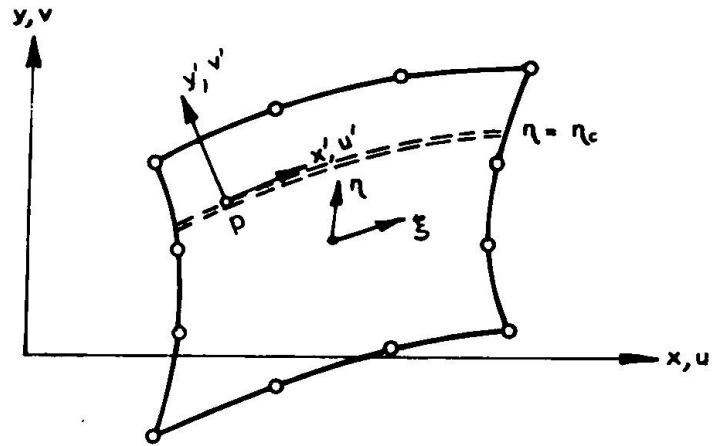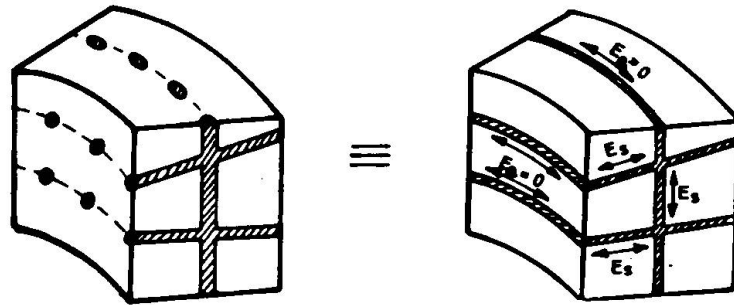
(i) RADIAL BARS

JACKET
OF
CABLES

≡

(ii) HOOP BARS

(b)

Fig. 1   Bar elements and axi-symmetric reinforcement
Fig. 1   Elements de barres et armaturage axi-symmétrique
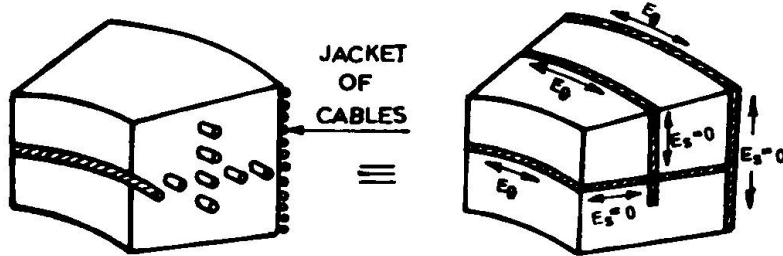Abb. 1   Stangeneisenbestandteile und axialsymmetrische Armierung

In this paper constitutive laws for concrete are presented which satisfy the requirement that the relationships should not be complex and should be based upon observations and results given by standard testing techniques. These laws are then incorporated into incremental non-linear finite element programs for the solution of plane and axisymmetric structures. Other inelastic effects such as creep and shrinkage of concrete, bond slip between steel and concrete, dowel action of reinforcing steel, etc., are not included. Point, bar and membrane elements are adopted to simulate bar reinforcement, liners, prestressing cables and jackets subject to the assumption that bending and shear resistance of such components can be ignored. Isoparametric elements, which have proved to be remarkably efficient in other non-linear applications, are exclusively employed and several solution algorithms are included in the programs.

In order to assess the techniques developed a realistic set of problems are solved and compared with experimental evidence. These include reinforced concrete beams, prestressed concrete pressure vessels, end plates in pressure vessels and slab-column junctions.

FINITE ELEMENTS FOR SIMULATION OF STEEL COMPONENTS

The use of the displacement method of finite element analysis is now well-known and will not be reproduced here. All the basic expressions can be found in Ref. [1] and the same notation will be employed in this paper.

A major advantage of isoparametric elements is that relatively few elements are required to idealize a given structure. Therefore in order to incorporate such details as reinforcing bars, prestressing cables (and sheets in axisymmetric cases) it is desirable to develop a line element which need not necessarily coincide with inter-element boundaries of the basic two-dimensional elements. Such a situation is illustrated in Fig. 1. The line of a bar lying along constant ξ or η direction is defined by using the same shape functions as the main element. Since full compatibility between bar and main element is assumed, the bar displacements are obtainable from the displacement field of the main element (for a bar running in the ξ direction) in the form

$$\begin{Bmatrix} u \\ v \end{Bmatrix} = \sum_{i=1}^{n} N_i \begin{Bmatrix} u_i \\ v_i \end{Bmatrix} \tag{1}$$

where n is the number of nodes per element. For bars only one component of strain contributes to the strain energy and is defined locally by

$$\varepsilon'_p = \frac{\partial u'}{\partial x'} \tag{2}$$

where x',y' are the local coordinates with y' being normal to the line of the bar and u',v' are the corresponding displacements. Defining a distortion matrix $[j]$ as

$$[j] = \begin{bmatrix} \dfrac{\partial u}{\partial x} & \dfrac{\partial v}{\partial x} \\ \dfrac{\partial u}{\partial y} & \dfrac{\partial v}{\partial y} \end{bmatrix} = [J]^{-1} \begin{bmatrix} \dfrac{\partial u}{\partial \xi} & \dfrac{\partial v}{\partial \xi} \\ \dfrac{\partial u}{\partial \eta} & \dfrac{\partial v}{\partial \eta} \end{bmatrix} = [J]^{-1} \begin{bmatrix} \dfrac{\partial N_1}{\partial \xi} & \cdots & \dfrac{\partial N_n}{\partial \xi} \\ \dfrac{\partial N_1}{\partial \eta} & \cdots & \dfrac{\partial N_n}{\partial \eta} \end{bmatrix} \begin{bmatrix} u_1 & v_1 \\ \vdots & \vdots \\ u_n & v_n \end{bmatrix} \tag{3}$$

4.

where $[J]$ is the Jacobian matrix given by

$$[J] = \begin{bmatrix} \dfrac{\partial x}{\partial \xi} & \dfrac{\partial y}{\partial \xi} \\ \dfrac{\partial x}{\partial \eta} & \dfrac{\partial y}{\partial \eta} \end{bmatrix} = \begin{bmatrix} \dfrac{\partial N_1}{\partial \xi} & \cdots\cdots & \dfrac{\partial N_n}{\partial \xi} \\ \dfrac{\partial N_1}{\partial \eta} & \cdots\cdots & \dfrac{\partial N_n}{\partial \eta} \end{bmatrix} \begin{bmatrix} x_1, & y_1 \\ & \vdots \\ x_n & y_n \end{bmatrix} \tag{4}$$

we can write the expression for the strain tensor as

$$[\varepsilon] = \tfrac{1}{2}\{[j] + [j]^T\} \tag{5}$$

Therefore $[j]$ is a tensor and transforms upon coordinate rotation from x,y to x',y' according to

$$[j'] = \begin{bmatrix} \dfrac{\partial u'}{\partial x'} & \dfrac{\partial v'}{\partial x'} \\ \dfrac{\partial u'}{\partial y'} & \dfrac{\partial v'}{\partial y'} \end{bmatrix} = [R][j][R]^T \tag{6}$$

where $[R]$ is the rotation matrix of direction cosines at the point under consideration given by

$$[R] = \begin{bmatrix} \dfrac{\partial x}{\partial x'} & \dfrac{\partial y}{\partial x'} \\ \dfrac{\partial x}{\partial y'} & \dfrac{\partial y}{\partial y'} \end{bmatrix} = \dfrac{1}{\sqrt{\left[\dfrac{\partial x}{\partial \xi}\right]^2 + \left[\dfrac{\partial y}{\partial \xi}\right]^2}} \begin{bmatrix} \dfrac{\partial x}{\partial \xi} & \dfrac{\partial y}{\partial \xi} \\ -\dfrac{\partial y}{\partial \xi} & \dfrac{\partial x}{\partial \xi} \end{bmatrix} \tag{7}$$

since x' and ξ coincide and differ only in magnitude.

From (2), (6) and (7) it follows that the direct strain component in the direction tangential to the bar is

$$\varepsilon'_p = \dfrac{1}{\left[\dfrac{\partial x}{\partial \xi}\right]^2 + \left[\dfrac{\partial y}{\partial \xi}\right]^2} \begin{bmatrix} \{C_1 \dfrac{\partial N_1}{\partial x} + C_2 \dfrac{\partial N_1}{\partial y}\}, & \{C_2 \dfrac{\partial N_1}{\partial x} + C_3 \dfrac{\partial N_1}{\partial y}\}, & \cdots \end{bmatrix} \begin{Bmatrix} u_1 \\ v_1 \\ u_2 \\ v_2 \\ \vdots \end{Bmatrix} \tag{8}$$

where $C_1 = \left(\dfrac{\partial x}{\partial \xi}\right)^2$, $C_2 = \dfrac{\partial x}{\partial \xi}\dfrac{\partial y}{\partial \xi}$, $C_3 = \left(\dfrac{\partial y}{\partial \xi}\right)^2$ $\tag{9}$

This expression applies to a single bar in plane stress or a sheet in plane strain or axisymmetric problem. In the latter case there will be a further strain in the hoop direction defined simply by

$$\varepsilon_\theta = \dfrac{u}{r_p} = \dfrac{\displaystyle\sum_{i=1}^{n} N_i u_i}{\displaystyle\sum_{i=1}^{n} N_i r_i} \tag{10}$$

where r_p is the radius at point P. The finite element process then proceeds in the usual manner to obtain the stiffness and other matrices.

In axisymmetric analysis several types of reinforcement are encountered. Besides isotropic sheets, these include reinforcement and cables lying in the plane of the axis of symmetry and reinforcement and cables lying in the hoop direction. These can be represented by equivalent anisotropic sheets by making appropriate adjustments to the $[D']$ matrix. Below we list the alternatives:

1) For a steel sheet with anisotropic properties consistent with an axisymmetric condition the elasticity matrix is found to be

$$[D'] = \frac{1}{1-\nu_{\theta s}\nu_{s\theta}} \begin{bmatrix} E_s & \nu_{s\theta}E_s \\ \nu_{\theta s}E_\theta & E_\theta \end{bmatrix} \tag{11}$$

where E and ν are the elastic modulus and Poissons ratio respectively in the radial (s) and hoop (θ) directions.

2) Reinforcement and cables in radial planes can be idealized by a sheet material with no hoop stiffness resulting in

$$[D'] = E_s \begin{bmatrix} 1 & 0 \\ 0 & 0 \end{bmatrix} \tag{12}$$

3) Reinforcement and prestressing cables in the hoop direction may be modelled by a sheet with no stiffness in radial planes, giving

$$[D'] = E_\theta \begin{bmatrix} 0 & 0 \\ 0 & 1 \end{bmatrix} \tag{13}$$

A further special element is the single point element convenient for representing discrete bunches of circumferential prestressing cables. This avoids the numerical and mesh grading difficulties that would be encountered if the use of small conventional elements were attempted. The element stiffness can be calculated directly by considering the equilibrium of a circular hoop of material of radius R which is subjected to a radial displacement δ. It can be easily shown [2] that the tension developed in the cable is

$$F = K.\delta \tag{14}$$

where
$$K = \frac{2\pi EA}{R}$$

where E and A are the elastic modulus and cross-sectional area of the cable respectively.

SOLUTION TECHNIQUES FOR NON-LINEAR PROBLEMS

The process of application of the finite element method to problems involving non-linear material behaviour is well documented [3-12] and therefore only the essential steps are repeated below. Provided that the strains in the structure are small the non-linear analysis may be based on the elastic process of solution. In this the elastic problem is repeatedly solved and successive corrections applied until both equilibrium and the appropriate constitutive laws are finally satisfied. The constitutive laws are generally specified in the form

$$F(\{\sigma\}, \{\epsilon\}) = 0 \tag{15}$$

Consider an intermediate situation where equilibrium conditions have been established. During a further load increment, if an elastic solution is performed in place of a true non-linear analysis, it will be found that

$$\{\psi(\delta)\} = \int_V [B]^T \{\sigma\} dV - \{R\} \neq 0 \tag{16}$$

in which $\{R\}$ lists all the forces due to external loads, initial stresses, etc. and in which $\{\sigma\}$ are the actual stresses dependent on the strain level reached as governed by equation (15). The residual force vector $\{\psi\}$ can be visualized as additional nodal forces required to bring the assumed (elastic) displacement pattern into nodal equilibrium.

Since $\{R\}$ is independent of $\{\delta\}$ the variation in $\{\psi\}$ due to a change $d\{\delta\}$ can be calculated from (16) to be

$$d\{\psi\} = \int_V [B]^T d\{\sigma\} dV \tag{17}$$

If the constitutive law can be expressed in the form

$$d\{\sigma\} = \left[D_T(\{\epsilon\})\right] d\{\epsilon\} \tag{18}$$

then (17) can be rewritten as

$$d\{\psi\} = \left[K_T(\delta)\right] d\{\delta\} \tag{19}$$

where

$$\left[K_T(\delta)\right] = \int_V [B]^T \left[D_T(\{\epsilon\})\right] [B] dV \tag{20}$$

Solution can then be accomplished by starting from initial conditions corresponding to $\{\delta\}_o = 0$, calculating the residuals by means of (16) and then obtaining the correction to the displacements which, generally, is given by

$$\Delta\{\delta\}_n = - \left[K_T\right]_{n-1}^{-1} \{\psi\}_{n-1} \tag{21}$$

this iterative process being repeated until convergence is deemed to have occurred. This approach is immediately recognised as a generalized Newton-Raphson technique which however introduces numerical difficulties in strain-softening situations. Alternatively it is possible to proceed using a constant value for the incremental stiffness corresponding to the initial elastic stiffness $\left[K_o\right]$. The above procedure is then repeated with the general correction given by

$$\Delta\{\delta\}_n = - \left[K_o\right]^{-1} \{\psi\}_{n-1} \tag{22}$$

This process is termed the "initial stress method" [12] presented by Zienkiewicz et al [8] and has been shown to be unconditionally convergent by Argyris and Scharpf [13]. For situations where it is only possible to express the strains explicitly in terms of stress the elastic constitutive relation can be employed in conjunction with [16] to obtain the residual forces. The previous procedure is then repeated and is naturally termed the "initial strain method".

The computer time required per iteration in the initial stress method is obviously only a fraction of that required in the tangential stiffness technique. However convergence may be slow in the former approach when a large proportion of the structure behaves non-linearly. Therefore, in general, a combination of the two schemes is desirable with the element stiffnesses being updated at the beginning of a load increment but then kept constant during iteration to the non-linear solution. Improved convergence rates can be achieved by the use of accelerators where previous information is employed to make more accurate predictions of the displacements. Such techniques were utilized [11] in this study with the degree of success however being rather limited.

CONSTITUTIVE AND FAILURE LAWS FOR THE FINITE ELEMENT ANALYSIS OF REINFORCED CONCRETE

The laws for the constituent materials of reinforced concrete are developed separately with steel components being modelled directly in finite element analysis. Despite widespread use of structural concretê over a considerable period of time, there exists an incomplete state of knowledge regarding concrete behaviour under various stress combinations. For instance there is no universally accepted triaxial failure criterion under combinations of tensile and compressive stresses. Also, with a few exceptions, most tests under biaxial and triaxial stress have been preoccupied with strength characteristics to the exclusion of stress-strain relationships.

The primary cause of concrete non-linearity is undoubtedly due to tensile cracking. In this work this is modelled by both a maximum principal stress and maximum principal strain criterion. The stress-strain relationship is assumed to be linear until the largest tensile principal stress or strain attains its maximum limiting value (f_t' or ε_{cr} respectively). At this stage, a tensile crack is assumed to develop normal to this principal direction and from this moment the material is incapable of supporting any tensile stress in this direction. In the isoparametric element context a crack implies an infinite number of parallel fissures across the applicable part of the element. For any subsequent increase in load the crack direction is assumed to be unchanged and the concrete is capable of sustaining full load in directions parallel to the crack. The development of further cracks is restricted to directions perpendicular to the first crack, the point of initiation being determined from the tensile strain values in directions parallel to the original crack.

Although a crack may be open in a normal direction it is possible that aggregate interlocking will restrict any shear deformation of the crack surfaces. This frictional restraint will depend on the concrete properties and, since the condition of the crack surfaces will change with continuing sliding, also the loading history. In this study aggregate interlocking is taken into account by postulating the shear stress along the crack to be a linear function of the corresponding strain according to

$$\tau^* = a'G\gamma^* \qquad (27)$$

where G is the shear modulus of the original uncracked material and a' is some preselected constant with value $0 \le a' \le 1$

On further loading it is possible that a crack may close and it is assumed that the full compressive stress may be developed across the fissure. The shear resistance will depend on a number of factors, e.g. normal compressive stress, interface characteristics, etc., and the problem

8.

is analogous to that of interlocking. Consequently

$$\tau^* = a''G\gamma^* \qquad (28)$$

where $0 \le a'' \le 1$. It is difficult to assign realistic values to a" and in this work a" = 1 was used implying a perfect "healing" of the crack.

The onset of cracking will introduce orthotropic conditions and the normal elasticity matrix must be modified. In crack directions the stress-strain relationship becomes, for the plane strain case

$$\begin{Bmatrix} \Delta\dot{\sigma}_n^* \\ \Delta\sigma_t^* \\ \Delta\tau^* \end{Bmatrix} = [D_T]^* \begin{Bmatrix} \Delta\varepsilon_n^* \\ \Delta\varepsilon_t^* \\ \Delta\gamma^* \end{Bmatrix} \qquad (29)$$

where

$$[D_T]^* = \begin{bmatrix} 0 & 0 & 0 \\ 0 & E & 0 \\ 0 & 0 & a'G \end{bmatrix} \qquad (30)$$

and

$$\Delta\varepsilon_z^* = \frac{\nu}{E}\,\Delta\sigma_t^* \qquad (31)$$

Similar expressions hold for the cases of plane stress and axial symmetry. Before assembly of the overall stiffness matrix, these expressions have to be expressed globally by use of the normal transformation matrices.

Numerous experimental investigations into the behaviour of concrete under multi-axial stress have been undertaken by many workers using a variety of loading and testing conditions and an extensive review can be found in Ref. [14]. However only in the biaxial studies of Kupfer et. al. [15] and Weigler and Becker [16,17] were there any comprehensive strain measurements made. A detailed examination of these experimental results revealed that approximately unique relationships existed between volumetric strain and hydrostatic stress, and between deviatoric stress and strain, until close to failure. The deformational response in compression can then be simulated by assuming the tangent bulk modulus, K_T, and shear modulus, G_T, to be functions of the first and second stress invariants respectively, as follows

$$K_T = f_1(I_1) = f_1(\sigma_1 + \sigma_2 + \sigma_3)$$
$$G_T = f_2(J_2) = f_2([(\sigma_1-\sigma_2)^2 + (\sigma_2-\sigma_3)^2 + (\sigma_3-\sigma_1)^2]^{\frac{1}{2}}) \qquad (32)$$

The invariant relationships are obtained directly from available experimental curves. In the analysis the appropriate expressions (32) are introduced in a piecewise linear manner. At the beginning of a load increment values of K_T and G_T are evaluated from the current values of I_1 and J_2, which are then employed to evaluate the current tangential elasticity matrix $[D_T]$ which in turn is used to calculate the stress increment $\Delta\{\sigma\}$. This procedure however leads to divergence of the calculated stresses and strains from the specified constitutive law, and a corrective procedure is essential. Using the updated values of $\{\sigma\}$ intermediate values of G_T and K_T are predicted. The final values are then assumed to be a weighted mean of the values K_o, G_o at the start of the increment and the intermediate values K_i, G_i so that

$$G_F = G_i + C'(G_o - G_i)$$

$$K_F = K_i + C'(K_o - K_i)$$

(33)

where C' is a constant. Experience indicates C' = 0.6 to be the optimum value.

It is clear that the above deformation laws do not apply close to the ultimate load and that further assumptions need to be made to govern the collapse of the material. A number of criteria have been postulated for predicting failure under multiaxial compression. Two criteria which have found most acceptance are the Mohr-Coulomb hypotheses and the octahedral shearing stress theory. In biaxial stress situations the latter predicts experimental behaviour more closely than the former and for this reason the octahedral law is exclusively employed in this study. In this the octahedral shearing stress, τ_o, is limited according to some function of the octahedral normal stress, σ_o, so that

$$\tau_o \leq f(\sigma_o)$$

(34)

Experimental evidence indicates that good correlation is obtained by use of a linear relationship so that

$$\tau_o \leq C + n\sigma_o$$

(35)

where C and n are measured constants obtained from experimental results.

After peak stress has been recorded the material is considerably disrupted and the existence of a continuing stress-strain curve beyond this value indicates local redistribution of stresses after maximum strength is exceeded. In this study no detailed attempt is made at predicting behaviour after peak stress. The values of K_T and G_T are merely simultaneously reduced to relatively small values and the stress state is held constant at the peak values for increasing strain, in order to allow local redistributions to occur. Thus under uniaxial conditions, for instance, the stress-strain curve would exhibit a horizontal stress plateau after peak stress.

Steel components are assumed to obey the laws of classical plasticity with a Von Mises yield criterion being adopted. The Bauschinger effect is ignored and isotropic hardening of the material is allowed.

The above material laws were incorporated in a computer program employing isoparametric elements. Several solution algorithms were employed, including the tangential stiffness method, initial stress method and the combined approach previously advocated.

APPLICATIONS

Deep beams are frequently used members in complex structural systems and considerable research into their basic behaviour has been undertaken. Fig. 2(a) illustrates a singly reinforced deep beam which has been studied experimentally by Ramakrishnan et.al. [18]. With the span of the beam kept constant at 27 inches two depths of 15" and 30" were considered. In each case 12 parabolic elements were employed in solution and the reinforcement was approximated by bar elements lying on the bottom surface of the beam. The maximum tensile strain criterion for cracking was used and an aggregate interlock factor a' = 0.5 was adopted.
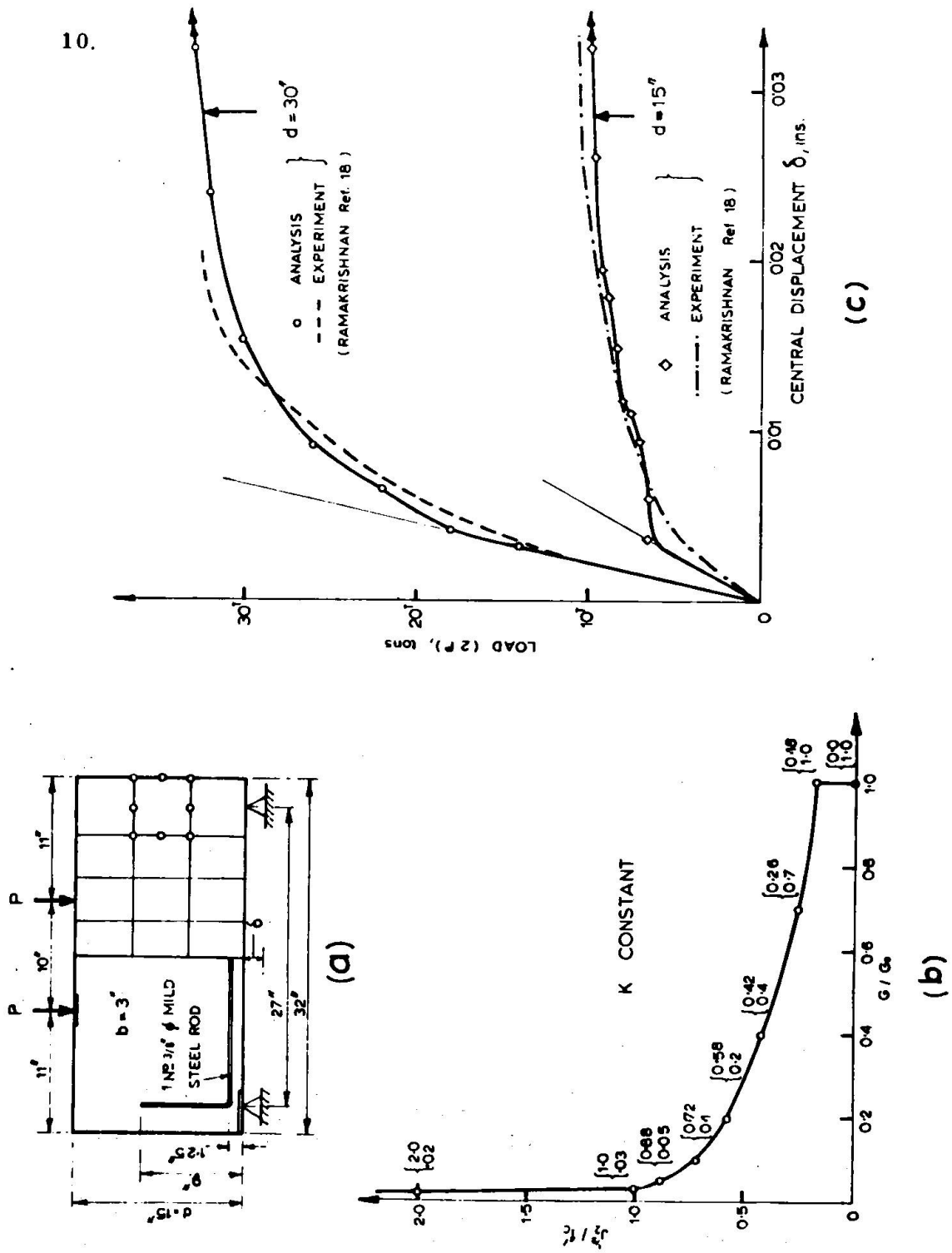
10.

Fig. 2 Singly reinforced deep beam under two point loading (a) Geometry
and finite element mesh employed; (b) Invariant compressive law assumed
in solution; (c) Load-displacement characteristics.

Fig. 2 Pontre épaisse à simple armature sous charge bi-ponctuelle
(a) Géométrie et maillage utilisés; (b) Loi de compression invariante
retenue dans la solution; (c) Caractéristiques charge-déplacement.

Abb. 2 Einseitig bewehrte wandartige Träger bei Belastung an zwei Punkten
(a) Geometrie und die Anwendun. von Gittern begrenzter Elemente; (b) Das
Gesetz des gleichbleibe. 'en Drucks wird für die Lösung angenommen;
(c) Charakteristika der Belastungsverteilung.

The invariant constitutive law was employed to simulate compressive behaviour and the relationship employed is shown in Fig. 2(b). The load-displacement characteristics are illustrated in Fig. 2(c) and good agreement between finite element and experimental results is evident.

The results of an exploratory investigation into the ultimate behaviour of a typical concrete dam on a rock foundation are presented in Fig. 3. The main geometrical features and dimensions of the dam correspond to the Norfolk dam analysed by Clough and Wilson [19]. The assumed loading system comprises water pressure on the upstream face and gravity loading in the dam and rock foundation. In order to produce ultimate conditions, an intuitive technique is used in which it is assumed that by increasing the weight of the dam and the water pressure (i.e. the density of the concrete and water) in proportion, it is approximately equivalent to gradually weakening the material. This process will cause associated stress redistribution which should eventually lead to the most probable failure mechanism.

The maximum strain criterion for cracking and the invariant constitutive law in compression were adopted for the concrete, whilst the rock system was assumed to be incapable of sustaining tension but to behave linearly in compression. The material properties employed are included in Fig. 3(a). Plane strain conditions were assumed and the parabolic element employed in solution. The zones of cracking and the principal stress distribution are shown in Fig. 3(a) and a reasonable distribution is obtained in spite of the coarse mesh employed. The displacement of the crest with increasing load is indicated in Fig. 3(b).

The next problem discussed is concerned with cylindrical prestressed concrete reactor vessels and corresponds to a model which had been previously tested [20,21]. The vessel had also been analysed using a lumped-parameter method [22,23] and these results offered a supplementary comparison. Details of the vessel (designated PV9) are given in Table 1 where the material properties assumed are also included. The prestressing system and the parabolic element mesh employed in solution are illustrated in Fig. 4. The vessel was first analysed for prestressing loads only; the prestressing system was then idealised by sheet elements and the vessel subjected to a steadily increasing internal pressure.

The pressure-deflection curve is shown in Fig. 4(a) where it can be seen that experiment is predicted remarkably well. Fig. 4(b) shows the variation of strains in the circumferential prestressing wire against internal pressure. Again, experimental behaviour is well predicted justifying the use of equivalent steel membranes.

Fig. 5(a) illustrates the tensile cracking of the vessel under increasing internal temperature whilst the redistribution of hoop stress with increasing temperature is illustrated in Fig. 5(b). This analysis did not account for the effects of temperature on material properties, a phenomenon which clearly needs to be included.

Further results of this study can be found in Refs. [2] and [14].

The next examples are concerned with the behaviour of end slabs of cylindrical pressure vessels and the problems considered had previously been the subject of an experimental investigation by Campbell-Allen and Low [24]. Slabs with thickness of 6" and 12" were
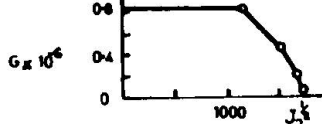
CONCRETE

ITIAL E = 2×10⁶ p.s.i

ITIAL V = 0.17

■ 3000 p.s.i.   K = 1·01 p.s.i. (CONSTANT)

:r ■ 0·00015

■ 62·5 p.c.f.

AX TENSILE STRAIN FOR CRACKING

:TAHEDRAL SHEAR STRESS FOR CRUSHING

$G \times 10^{6}$

0·8
0·4
0
1000 $J_2^{½}$

FISSURED ZONE

FISSURED ZONE

PRINCIPAL STRESSES AT 21×P

P — DESIGN LOAD

(GRAVITY AND WATER LOAD
PROPORTIONATELY INCREASED)

1 cm = 10,000 p.s.f.

δy

δx

(a)

ROCK

■ 5×10⁶ p.s.i.

■ 0·0
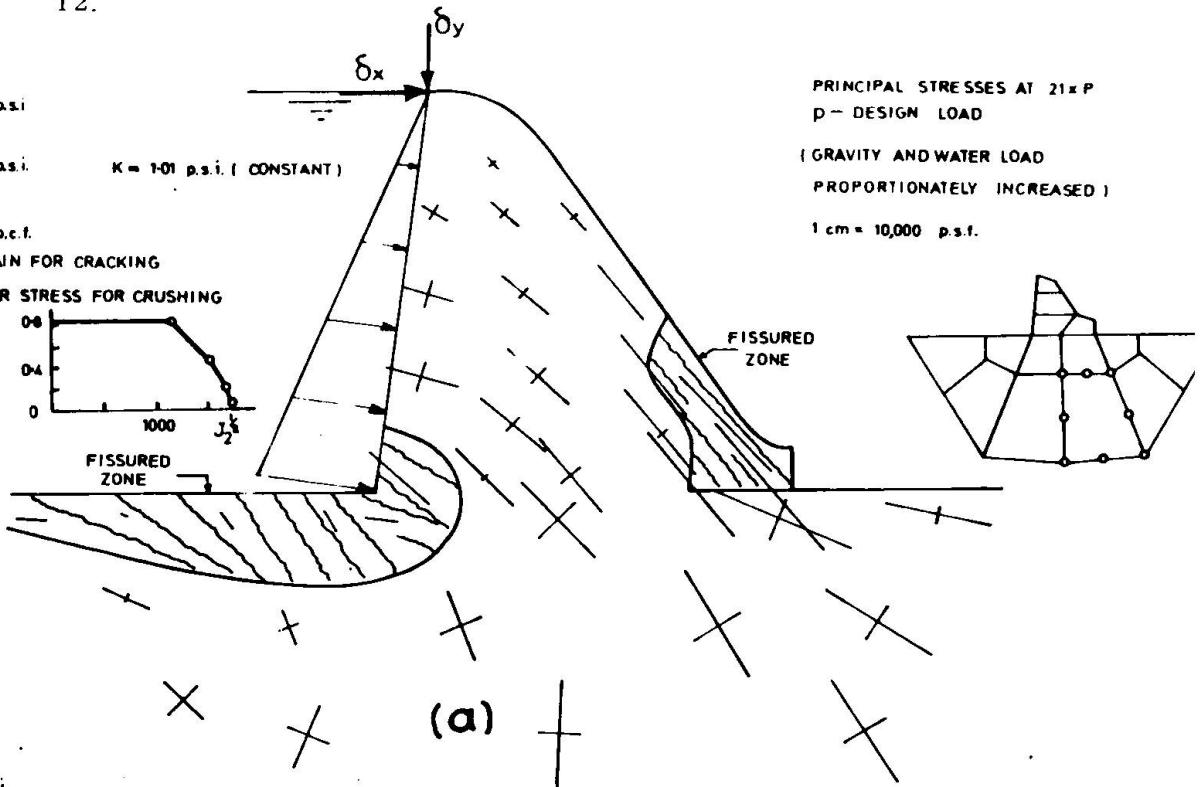
R ■ 62·5 p.c.f.

NO TENSION
LINEAR COMPRESSIVE LAW

LOAD

30 p

20 p

10 p

0

-0·2   -0·4   -0·6   -0·8   -1·0

DISPLACEMENT δ_x, ft

30 p
20 p
10 p

LOAD

0·4   0·2   0   -0·2
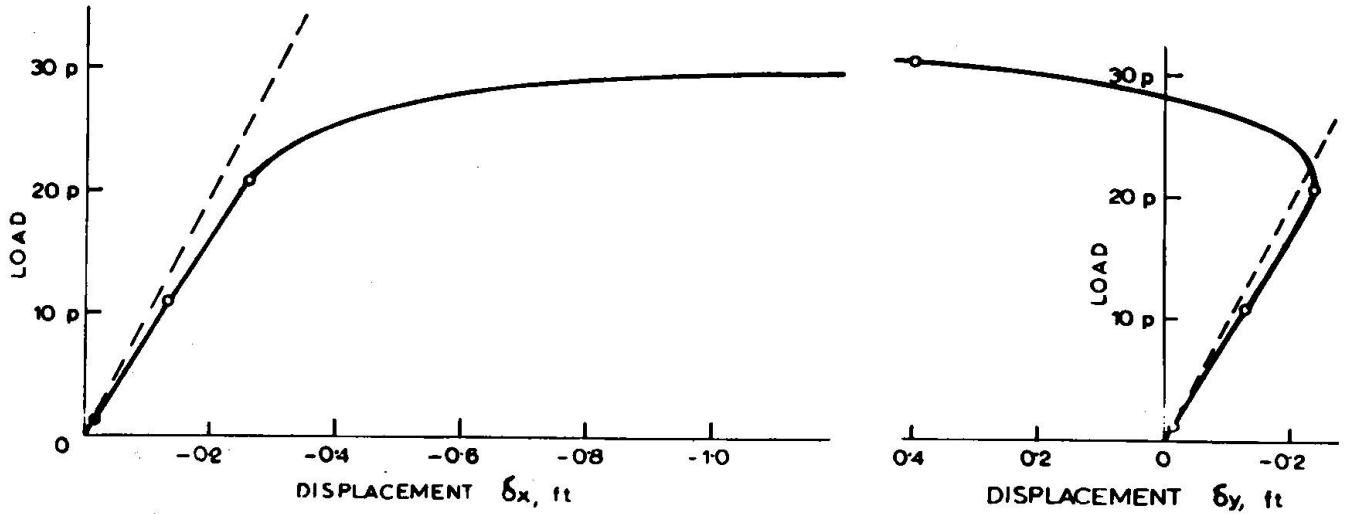
DISPLACEMENT δ_y, ft

(b)

Fig. 3 Ultimate behaviour of a gravity dam (a) Cracking and principal stress patterns; (b) Displacement of crest with increasing load.

Fig. 3 Comportement ultime d'un barrage-poids (a) Distribution des fissures et des contraintes principales; (b) Variation du déplacement de crête sous charge croissante.

Abb. 3 Endgültiges Verhalten einer Schwergewichtsmauer (a) Muster der Bruchstellen und der hauptsächlichen Belastungspunkte;

· (b) Verlagerung des Scheitelwertes bei zunehmender Belastung.

TABLE 1   DETAILS OF PRESSURE VESSEL PV9

|	PV9
External diameter	3'-4"
Height	6'-8"
Slab thickness, t_s	9"
Wall thickness, t_w	5"
Area of longitudinal cable	0.151 in^2
Area of hoop cable	0.029 in^2
Stress in long. cable	167 ksi
Stress in hoop cable	144 ksi
Yield stress of long. cable	225 ksi
Yield stress of hoop cable	225 ksi
Equivalent long. load	756 kips
Equivalent hoop pressure	510 psi
E_s	28×10^6 psi
Thickness of long. membrane	.036 in.
Thickness of hoop membrane	.042 in.
E_c	4.3×10^6 psi
ν_o	0.15
G_o	1.87×10^6 psi
K_o	2.05×10^6 psi
f_c'	7300 psi
$f_{t\bullet}'$	645 psi
ε_{cr}	.00015
c	2200 psi
n	0.63

14.

(a)

(b)
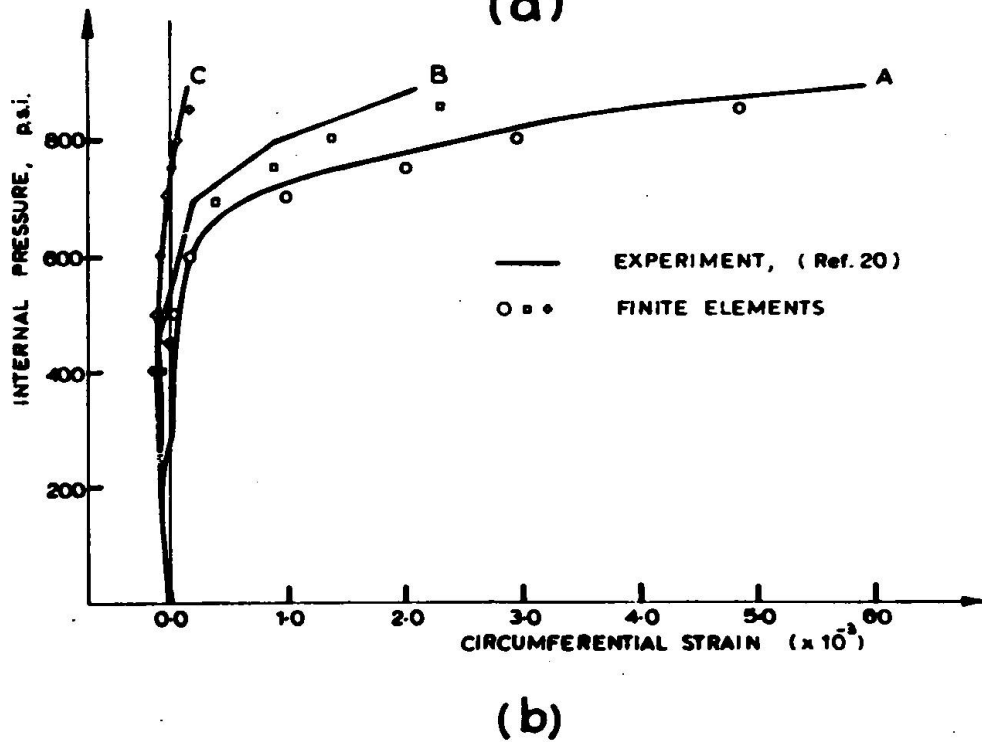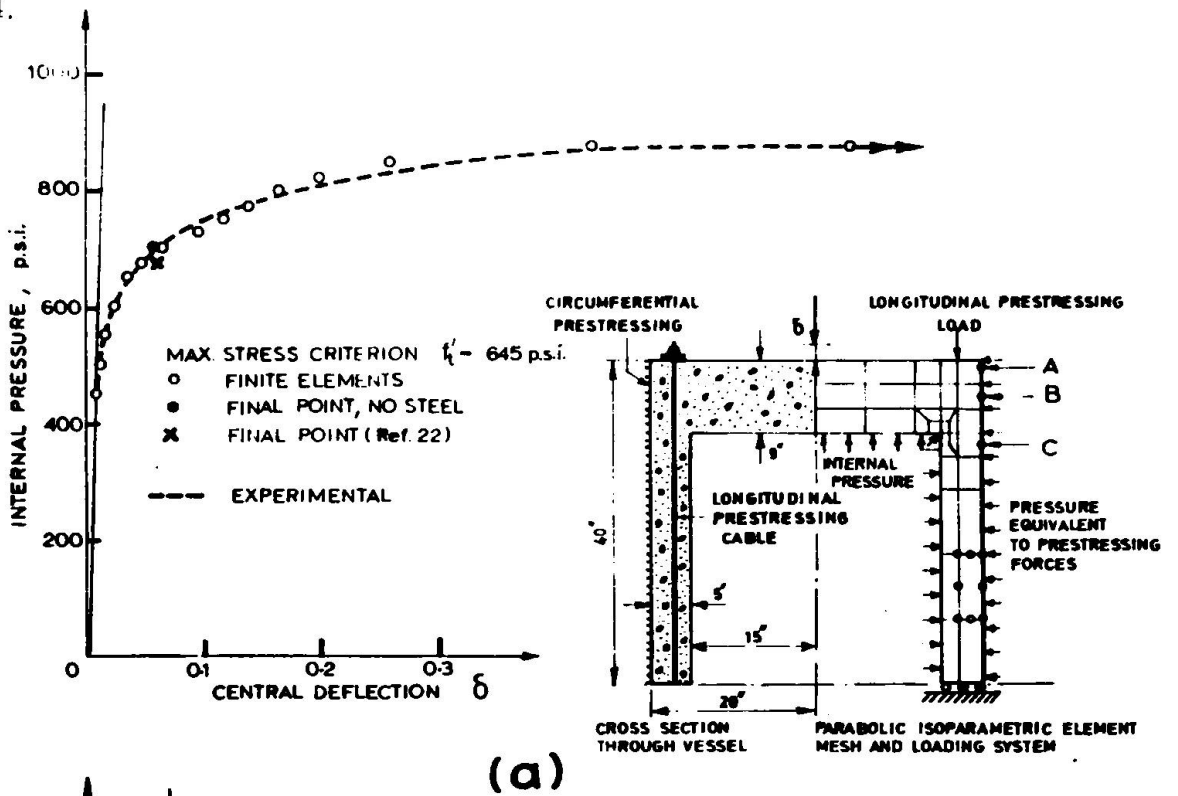
Fig. 4 Prestres ed pressure vessel PV9 under internal pressure
(a) Deflection of end-slab with increasing pressure; (b) Variation of strains in circumferential prestressing cables with increasing pressure.

Fig. 4 Enceinte de pressurisation précontrainte PV9 sous pression interne
(a) Déflection de la dalle d'extrémité sous pression croissante;
(b) Variation des déformations des câbles annulaires de précontrainte sous pression croissante.

Abb. 4 Vorgespannter Druckbehälter PV9 bei internem Druck (a) Nachgeben der Enddecke bei zunehmendem Druck; (b) Veränderung der Materialspannung ummantelter vorgespannter Stahldrähte bei ansteigendem Druck.
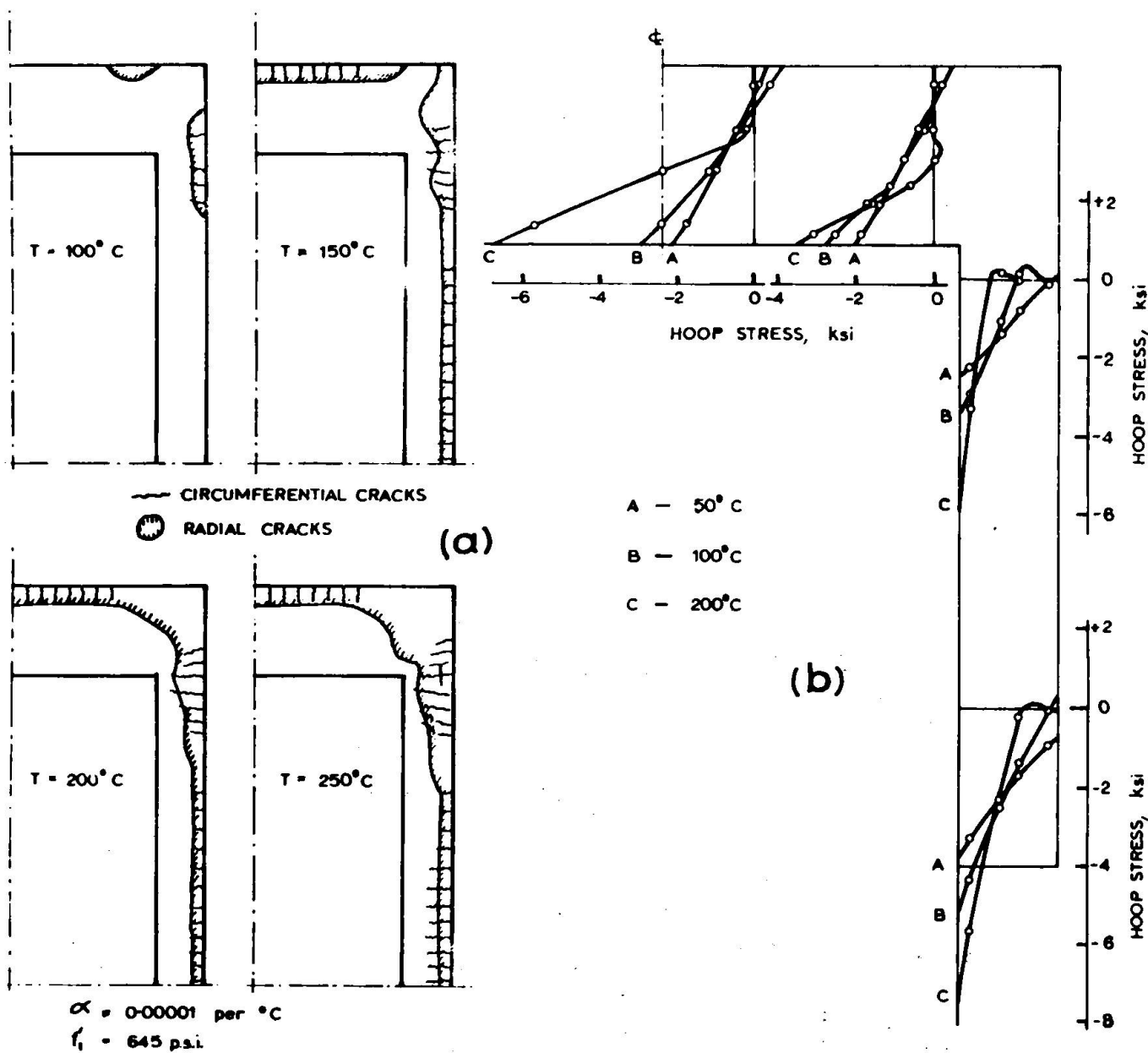
T - 100° C

T - 150°C

CIRCUMFERENTIAL CRACKS

RADIAL CRACKS

(a)

T - 200° C

T - 250°C

α = 0-00001 per °C

f₁ - 645 p.s.i.

HOOP STRESS, ksi

-6   -4   -2   0 -4   -2   0

A — 50° C

B — 100°C

C — 200°C

(b)

HOOP STRESS, ksi

Fig. 5 Thermal cracking of pressure vessel PV9 (a) Development of
tensile cracked zones with increasing temperature; (b) Change in hoop
stress di tribution with increasing temperature.

Fig. 5 Fissuration thermique d'une enceinte PV9 (a) développement des
zones de fissuration de tension sous température croissante; (b) Variation
de la distribution des contraintes annulaires sous température croissante

Abb. 5 Thermische Bruchstellen des Druckbehälters PV9 (a) Entwicklung
dehnbarer Bruchzonen bei steigenden Temperaturen; (b) Wechsel in der
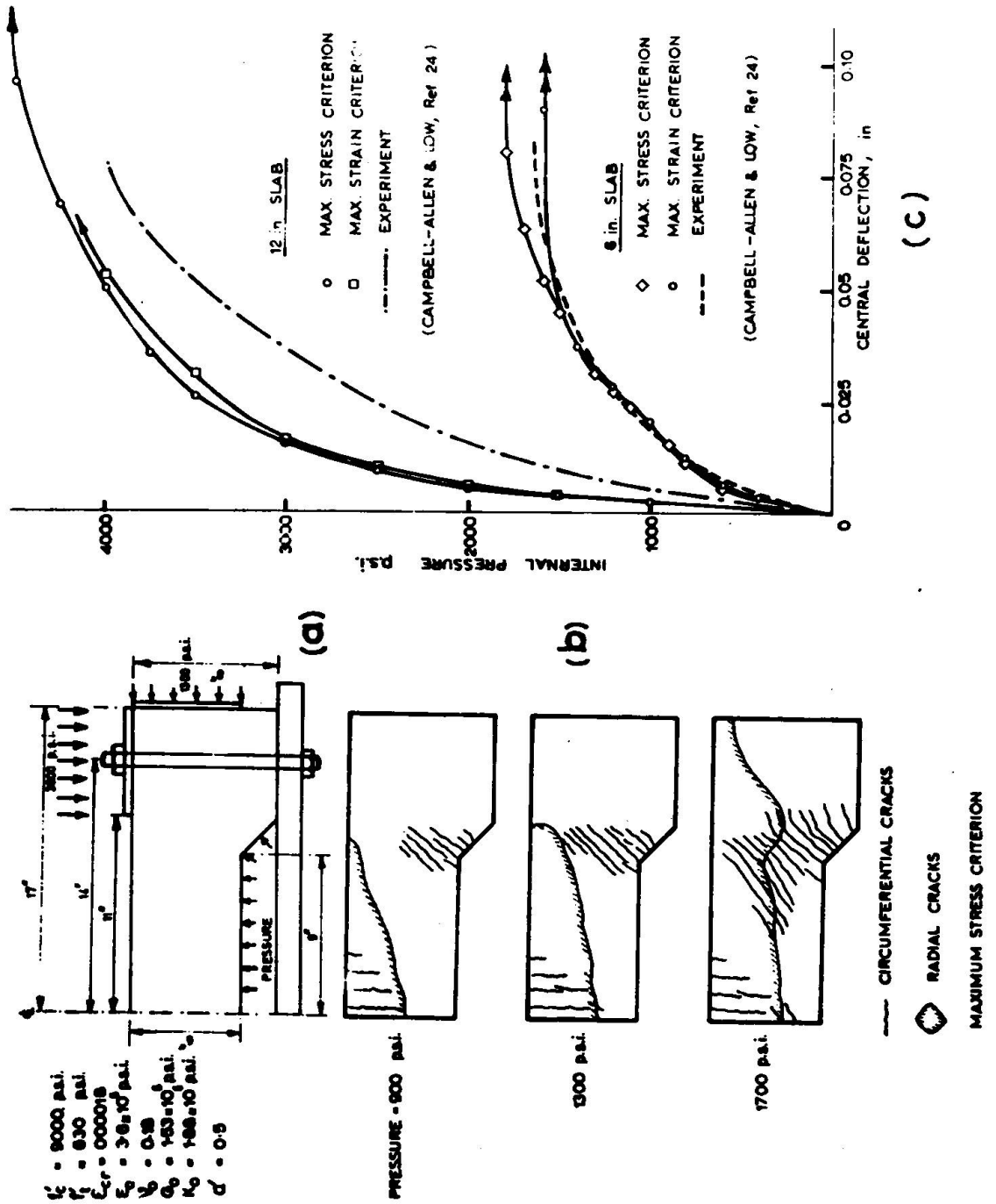Verteilung der Bandbelastung bei steigenden Temperaturen.

Fig. 6 Pressure vessel end-slab under pressure loading (a) Material properties, loading and geometry; (b) Development of cracked zones with increasing pressure (6" slab); (c) Central deflection of slabs with increasing pressure.

Fig. 6 Dalle de fermeture d'enceinte de pressurisation sous pression croissante (a) Propriétés mécaniques, chargement et géométrie; (b) Propagation des zones fissurées sous pression croissante (dalle de 15 cm d'epaisseur); (c) Déflection centrale des dalles sous pression croissan

Abb. 6 Enddecke des Druckgefässes bei Belastung durch Druck (a) Eigenschaft des Materials, Belastung und Geometrie; (b) Entwicklung der Bruchzonen bei zunehmendem Druck (sechs 'inch' Decke); (c) Nachgeben der Decken im Zentrum bei zunehmendem Druck.

analysed and the dimensions of the 6" thick slab and material properties assumed are shown in Fig. 6(a). The invariant compressive law was employed with K assumed constant. The variation of G with J_2^2 is the same as that shown in Fig. 2(b). The development of cracked zones in the 6" slab with increasing pressure is illustrated in Fig. 6(b), where, in addition to flexure of the end plate, there is evidence of a punching shear type of failure. The pressure-deflection curves are shown in Fig. 6(c) and the numerical results are in good agreement with the experimental values for the 6" slab. However, in the case of a 12" thick slab the correlation is not so good with the stiffness and ultimate load being overestimated by the finite element method.

The final problem studied was the behaviour of the slab-column junction previously considered by Andersson [25] which is illustrated in Fig. 7(a). Also shown is the reinforcement and the finite element mesh employed in analysis. The invariant compressive law was adopted again assuming the material properties indicated in Fig. 2(b) and the aggregate interlock factor a' was chosen as 0.5. Fig. 7(b) compares the numerical and experimental strain at a particular position in the shear reinforcement and it is seen that the agreement is good considering the complexity of the problem.

CONCLUDING REMARKS

It has been shown how the finite element method can be applied to solve problems of non-linear reinforced-concrete behaviour. By idealizing the steel and concrete constituents separately more realistic representation of the individual constitutive laws can be made. An attempt has been made at developing a constitutive law for concrete under multiaxial compressive stress by basing the material action on the hydrostatic and octahedral behaviour. Explicit expressions are obtained from a consideration of previous experimental results. The applicability or otherwise of this model is inconclusive since for most of the examples considered failure was primarily due to tensile cracking. It should also be emphasised that the compressive relationships are based on relatively little data, which in itself is subject to the many factors affecting the behaviour of concrete. However the approach merits further investigation as the laws obtained are relatively simple and can be readily employed in analysis.

On the other hand the criteria employed to describe tensile cracking appear to be well justified, with the numerical results generally being in good agreement with experimental values when failure is induced by this phenomenon. Further research is however necessary to investigate aggregate interlocking, shear resistance developed on crack closing, etc.

With regard to the numerical aspect of the method further work is necessary to determine the optimum solution algorithm. Present experience indicates that best convergence rates are obtained by use of a combination of tangential stiffness and initial stress techniques. The use of accelerators to improve convergence met only with limited success; the abrupt changes in local stress levels encountered during cracking making a forward prediction of the displacements difficult.

A possible alternative method of investigating basic concrete behaviour is offered by the overlay concept [26]. In this the material considered is assumed to be composed of several layers, or overlays, each of which may have different material properties or obey a different constitutive law. The summation of the contribution of each layer, in
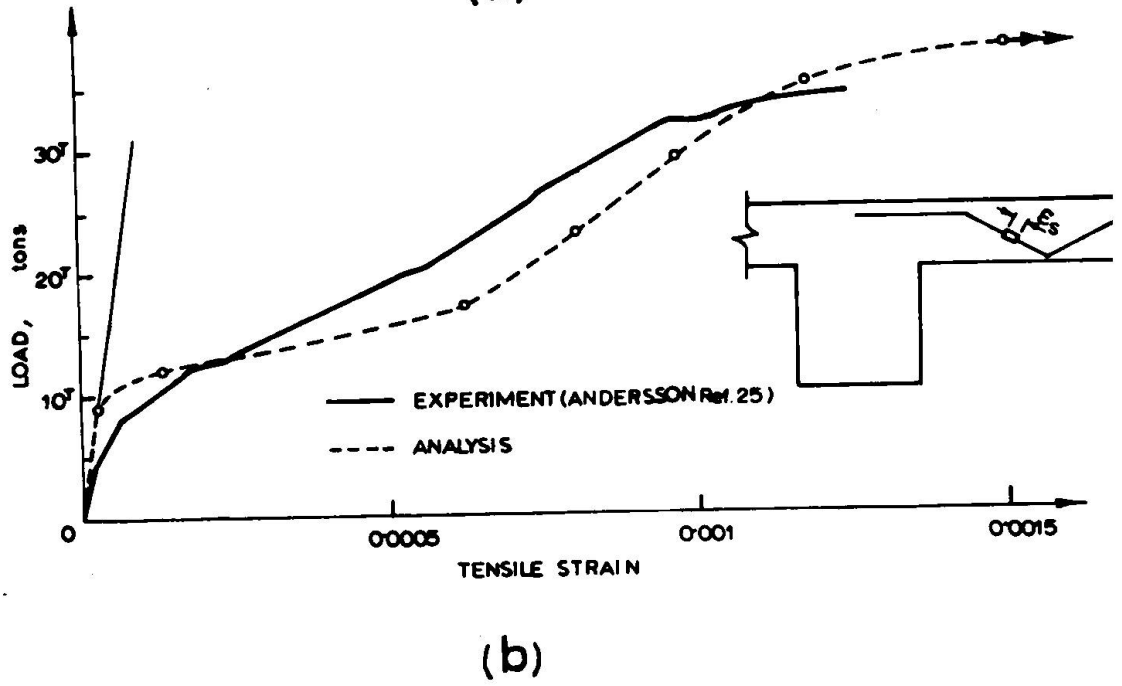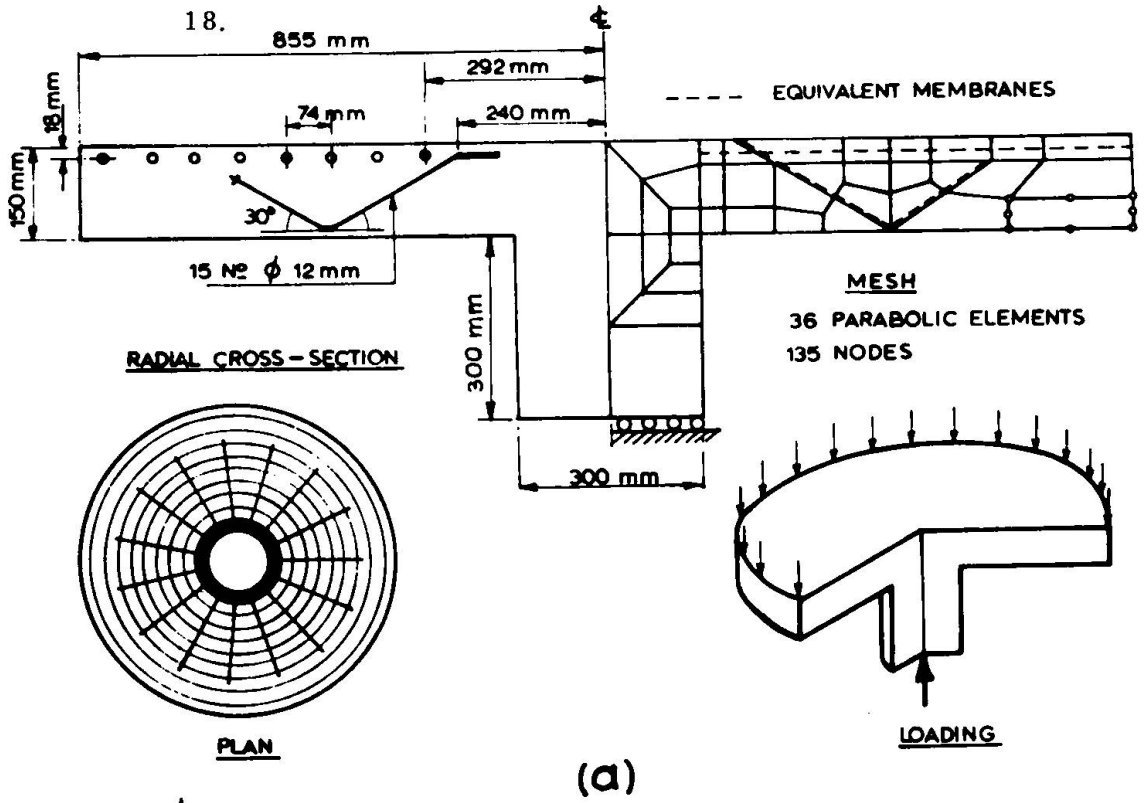
Fig. 7 Ultimate behaviour of a slab-column junction (a) Slab-column geometry illustrating reinforcement and finite element mesh employed; (b) Strain variation in shear reinforcement with increasing load.

Fig. 7 Comportement limite d'un accord dalle-colonne (a) Géométrie d'une jonction dalle-colonne illustrant l'armaturage et le maillage d'elements finis utilisé; (b) Variation des déformations dans l'armatur de cisaillement sous charge croissante.

Abb. 7 Endgültiges Verhalten einer Verbindung von Decke und Säule (a) Geometrie einer Decke und Säule, die Anwendung der Armierung und di Anwendung von Gittern begrenzter Elemente darlegt; (b) Verändergung de Materialspannung bei einer Armierung durch Schubkraft mit zunehmender Belastung.

some predetermined proportion, will then reproduce the overall material response. This immediately suggests that the microscopic behaviour of concrete can be examined by modelling each phase of the material (e.g. mortar, aggregate, etc.) by separate overlays. Such results could then be employed to develop macroscopic constitutive laws.

An important aspect of concrete which has been neglected in the present study is its creep behaviour. This phenomenon is important in many situations particularly if elevated temperatures are involved, as in nuclear pressure vessels. The overlay model appears to offer possibilities in this area also. Time-dependent behaviour can be introduced by use of visco-plastic [27,28] layers with the load shedding associated with tensile cracking being simulated either by assigning strain-softening characteristics to the material or including elastic overlays obeying a limiting tensile stress or strain criterion.

REFERENCES

1. ZIENKIEWICZ, O. C., "The Finite Element Method in Engineering Science" McGraw-Hill, 1971.

2. ZIENKIEWICZ, O. C., OWEN, D. R. J., PHILLIPS, D. V., NAYAK, G. C., "Finite element methods in the analysis of reactor vessels" Nuclear Engng. and Design, Vol. 20, No.2, 1972.

3. ODEN, J. T., "Finite element applications in non-linear structural analysis" Proc. Symp. on Applications of FEM in Civil Engineering, ASCE, Vanderbilt Univ., 1969.

4. MARCAL, P. V., KING, I. P., "Elastic-plastic analysis of two dimensional stress systems by the finite element method" Int. Journal Mech. Sci., Vol. 9, 1967, pp. 143-155.

5. GALLAGHER, R. H., PADLOG, J., BIJLARD, P. B., "Stress analysis of heated complex shapes", Journal Am. Rocket Soc., v.32, May 1962, pp. 700-707.

6. ARGYRIS, J. H., "Elasto-plastic matrix displacement analysis of three dimensional continua" Journal Roy. Aer. Soc., Vol. 69, 1965, pp. 633-635.

7. ZIENKIEWICZ, O. C., VALLIAPPAN, S., KING, I. P., "Stress analysis of rock as a 'no-tension' material" Geotechnique, Vol. 18, No. 1, 1968, pp. 56-66.

8. ZIENKIEWICZ, O. C., VALLIAPPAN, S., KING, I. P., "Elasto-plastic solutions of engineering problems; initial stress finite element approach" Int. Journal Num. Meths. Engng., Vol. 1, 1969, pp. 75-100.

9. ZIENKIEWICZ, O. C., and NAYAK, G. C., "A general approach to problems of large deformation and plasticity using isoparametric elements" Proc. 3rd Conf. Matrix Meths. Struct. Mech. Wright-Patterson A.F. Base, Ohio, (1971).

10. NAYAK, G. C., and ZIENKIEWICZ, O. C. "Elasto-plastic stress analysis. Generalization for various constitutive relations including strain softening" Int. J. Num. Meths. Engng. 1, p.75 (1969).

11. NAYAK, G. C., ZIENKIEWICZ, O. C., "Note on the 'alpha'-constant stiffness method for the analysis of nonlinear problems"

12. ZIENKIEWICZ, O. C., VALLIAPPAN, S., KING, I. P., "Elasto-plastic solutions of engineering problems; initial stress finite element approach" Int. Journal Num. Meths. Engg. Vol. 1, 1969, pp. 75-100.

13. ARGYRIS, J. H., and SCHARPF, D. W., "Methods of elasto-plastic analysis" ISD, ISSC Symp. on Finite Element Tech., Stuttgart, (1969).

14. PHILLIPS, D. V., "Non-linear analyses of structural concrete by finite element methods" Ph.D thesis, University of Wales, (1973).

15. KUPFER, H., HILSDORF, H. K., RUSCH, H., "Behaviour of concrete under biaxial stresses" Journal ACI, Vol. 66, No. 8, Aug. 1969, pp. 656-666.

16. WEIGLER, H., BECKER, G., "Uber das bruch und verformungsver-halten von beton bei mehrachsiger beanspruchung" Der Bauingenieur, 1961, Heft 10, pp. 390-396.

17. WEIGLER, H., BECKER, G., "Untersuchungen uber das bruch und verformungsverhalten von beton bei zweiachsiger beanspruchung" Berlin 1963, Heft 157, des Deutschen Ausschusses fur Stahlbeton.

18. RAMAKRISHNAN, V., ANATHANARAYANA, Y., "Ultimate strength of deep beams in shear" Journal ACI, V65, No. 2, Feb. 1968, pp. 87-98.

19. CLOUGH, R. W., WILSON, E. L., "Stress analysis of a gravity dam by the finite element method" Bulletin RILEM, No. 19, pp. 45-54, June 1963.

20. SOZEN, M. A., PAUL, S. L., "Structural behaviour of a small scale prestressed reactor vessel" Nucl. Engng. and Design, V.8, 1968, pp. 403-414.

21. PAUL, S. L., et. al. "Strength and behaviour of prestressed concrete vessels for nuclear reactors, Volumes I and II" Civil Engng. Studies, Structural Research Series No. 346, University of Illinois, Urbana, Illinois, July 1969.

22. MOHRAZ, B., SCHNOBRICH, W. C., GOMEZ, A. E., "Crack development in a prestressed concrete reactor vessel as determined by a lumped parameter method" Nucl. Engng. and Design, Vol. 11, 1970, pp. 286-294.

23. GOMEZ, A. E., SCHNOBRICH, W. C., "Lumped parameter analysis of cylindrical prestressed concrete reactor vessels" Civ. Eng. Studies, Structural Research Series No. 340, University of Illinois, Urbana, Illinois, Dec. 1968.

24. CAMPBELL-ALLEN, D., LOW, E. W. E., "Pressure tests on end slabs for prestressed concrete pressure vessels" Nucl. Engng. and Design, V.6, 1967, pp. 345-359.

25. ANDERSSON, J. L., "Punching of concrete slabs with shear reinforcement" Transactions, Royal Institute of Technology, No. 212, Stockholm, 1963.

26. ZIENKIEWICZ, O. C., NAYAK, G. C., OWEN, D. R. J., "Composite and overlay models in numerical analysis of elasto-plastic continua" Int. Symp. Foundations of Plasticity, Warsaw, Poland, Sept. 1972.

27. ZIENKIEWICZ, O. C., and CORMEAU, I. C., "Visco-plasticity
     solution by the finite element process" Archives of Mechanics,
     24, 5-6, pp. 873-889, (1972).

28. ZIENKIEWICZ, O. C., OWEN, D. R. J. and CORMEAU, I. C., "Analyses
     of visco-plastic Effects in pressure Vessels by the finite element
     method" 2nd Int. Conf. on Struct. Mechanics in Reactor Technology,
     Berlin (1973).

SUMMARY

        This paper is concerned with the application of the finite
element technique to the solution of reinforced concrete and plain concrete
structures. It is assumed that non-linear response is solely due to
tensile cracking and multiaxial compressive response of the concrete and
to yielding of the steel reinforcement. The effects of aggregate inter-
locking along crack surfaces are briefly considered. The analysis is
restricted to plane and axisymmetric situations and special purpose
elements are introduced to simulate steel reinforcement, liners, pre-
stressing systems, etc. Constitutive and failure laws are presented
and incorporated into incremental non-linear finite element computer
programs. The isoparametric element concept is exclusively employed.
To assess the methods developed, a realistic set of problems are solved
and compared with experimental evidence.

RÉSUMÉ

        Cet article concerne l'application de la technique des
éléments finis a l'étu de structures en béton massif ou armé. On
suppose que le comportement non-linéaire est dû uniquement à la réponse du
béton par fissuration sous tension et sous compression multiaxiale ainsi
qu'à la plastification des armatures. Les effets de blocage dûs aux
agrégats le long des fissures sont brièvement considérés. L'analyse se
limite aux situations planes et axi-symétriques et des éléments
spécialisés sont introduits pour simuler armatures, gaines, dispositifs de
précontrainte, etc. Les équations constitutives et critères de rupture
sont présentés et incorporés dans des programmes d'éléments finis
non-linéaires. On retient exclusivement le concept de l'élément
isoparamétrique. Un ensemble de problemes concrets est résolu; la
comparaison avec les observations expérimentales fermet l'évaluation des
méthodes proposées.

ZUSAMMENFASSUNG

        In diesem Beitrag werden Aussagen über die Anwendung der
Technik begrenzter Elemente zur Schaffung bewehrter Betonstrukturen und
solche zur Schaffung nichtbewehrter Betonstrukturen gemacht. Es wird davon
ausgegangen, dass nichtlineares Verhalten ausschliesslich auf Dehnungs-
spannungen und das Verhalten bei mehrachsiger Druckbeanspruchung innerhalb
des Betons zurückzuführen ist, sowie auf ein Nachgeben der Stahlarmierung.
Die Auswirkungen der Verblockung von Aggregaten entlang den Oberflächen
der Bruchzonen werden kurz berücksichtigt. Die Analyse beschränkt sich
auf ebene und axialsymmetrische Situationen. Elemente, die einem besonderen
Zweck dienen, werden verwendet, um Stahlbewehrungen, Einlegerohre,
vorgespannte Systeme, usw. zu simulieren. Konstitutive Gesetze und solche
des Versagens werden dargelegt und in zusätzliche Komputerprogramme
nichtlinearer endlicher Elemente aufgenommen. Die Konzeption gleicher
Parameterbestandteile wird ausschliesslich angewandt. Eine Anzahl
tatsächlich bestehender Probleme wird gelöst und mit experimentellen
Beweisen verglichen. Dies soll als Grundlage für die Beurteilung der
entwickelten Methoden dienen.

Leere Seite

Blank page

Page vide